



# A physical model for metal extraction and transport in shallow magmatic systems

**Christian Huber**

*School of Earth and Atmospheric Sciences, Georgia Institute of Technology, Atlanta, Georgia 30332, USA (christian.huber@eas.gatech.edu)*

**Olivier Bachmann**

*Department of Earth and Space Sciences, University of Washington, Seattle, Washington 98105, USA*

**Jean-Louis Vigneresse**

*G2R, Nancy-Université, BP 23, FR-54501 Vandoeuvre CEDEX, France*

**Josef Dufek**

*School of Earth and Atmospheric Sciences, Georgia Institute of Technology, Atlanta, Georgia 30332, USA*

**Andrea Parmigiani**

*Computer Science Department, University of Geneva, CH-1211 Geneva, Switzerland*

[1] The highest concentrations of metals (e.g., Cu, Au, Ag, Mo) in the Earth's crust are found in porphyry-type deposits. The metals are ultimately sourced from magmas, and appear to be concentrated hundred to thousand-fold from typical magmatic contents (ppm-ppb) in the exsolved volatile phase. To better quantify the purging and transport of metals, we develop a physical model of volatile evolution in an incrementally built upper crustal magma reservoirs that considers (1) partitioning of metals from the melt to an exsolved volatile phase, and (2) advection of the buoyant volatile phase using a single dimensionless parameter, the Péclet number ( $Pe$ ; ratio of advection rate over diffusion rate). We propose that metal extraction and segregation from magmas can occur in 3 stages with different  $Pe$ : (1) during exsolution of the magmatic volatile phase in shallow, crystal-poor magma bodies (slow volatile advection;  $Pe \ll 1$ ), (2) during the growth of volatile channels that develop in the reservoir as crystallinity increases ( $Pe < 1$ ), and (3) during advection in connected channels (rapid volatile advection, high  $Pe \geq 1$ ). For each stage, a metal enrichment factor can be calculated, allowing insight into the optimal conditions to maximize metal mass flux into the overlying hydrothermal system. The model predicts that the most efficient purging of metals occurs for magmas with intermediate volatile contents and is enhanced during late-stage magmatic activity, as the reservoirs reach high crystallinity and are not disturbed by volcanic venting, in agreement with natural observations suggesting that ore formation post-dates volcanic activity.

**Components:** 10,100 words, 11 figures, 2 tables.

**Keywords:** economic geology; fluid exsolution; magma reservoir; metals enrichment; porphyry-copper deposits.

**Index Terms:** 1036 Geochemistry: Magma chamber processes (3618); 8424 Volcanology: Hydrothermal systems (0450, 1034, 3017, 3616, 4832, 8135); 8430 Volcanology: Volcanic gases.

**Received** 11 January 2012; **Revised** 21 May 2012; **Accepted** 26 June 2012; **Published** 9 August 2012.

Huber, C., O. Bachmann, J.-L. Vigneresse, J. Dufek, and A. Parmigiani (2012), A physical model for metal extraction and transport in shallow magmatic systems, *Geochem. Geophys. Geosyst.*, 13, Q08003, doi:10.1029/2012GC004042.

## 1. Introduction

[2] Most of the metals used in our society ultimately originate from magmas generated by igneous processes. However, concentrations of metals are low in any magma (e.g., ~30 ppm for Cu and a few ppb for Au and Ag in the average upper crust [Rudnick and Gao, 2003]). For mining to be economically viable, large enrichments need to be achieved. Understanding the processes that lead to these enrichments is of obvious importance for the mining industry and our society at large.

[3] Upper crustal magma chambers that typically underlie porphyry-type deposits consist of silicate melt, multiple crystalline phases and a magmatic volatile phase (MVP, which may be any of the following: a supercritical fluid, a low-density vapor phase, and/or higher density saline liquid and is made of H<sub>2</sub>O, CO<sub>2</sub>, sulfur compounds and halogens [Webster et al., 2009]). Such a MVP exsolves from the silicate melt as a consequence of two different processes known as first and second boiling [e.g., Burnham, 1979; Candela, 1997]: *first boiling* occurs during magma ascent, owing to an increase in partial pressure of volatiles dissolved in the melt with decompression whereas *second boiling* occurs during cooling of the magma, as crystallization proceeds at constant pressure, leading to an increase in volatile elements and saturation in the melt phase.

[4] Due to its low viscosity and strong miscibility with surface waters and the atmosphere, the MVP is not commonly preserved in the rock record; it can only be isolated and sampled in (1) hot fumaroles in active volcanoes and (2) in fluid inclusions trapped in crystals in igneous rocks. When metals are measured in such fluids, concentrations are up to 2–3 orders of magnitude higher than in associated host rocks [Taran et al., 2000; Halter et al., 2002; Harris et al., 2003; Williams-Jones and Heinrich, 2005; Zelenski and Bortnikova, 2005]. Hence, it appears likely that the MVP (including both brine and vapor) is the carrier of metals from the magmas to the hydrothermal system [Hedenquist and Lowenstern, 1994], although it is possible that, in some cases, an immiscible sulfide melt phase (trapped in some magmatic phenocrysts [e.g., Halter et al., 2002; Nadeau et al., 2010; Naldrett, 2004; Chung and Mungall, 2009; Muntean et al., 2011]) can exsolve at depth and strongly

sequester chalcophile elements (Cu, Au). However, in water-rich arc environments, exsolution of MVP is expected to destabilize this sulfide melt and inherit its metal-rich composition [Nadeau et al., 2010; Scaillet, 2010].

[5] The processes leading to the concentration of metals in MVP and their transport out of the parental magma body are complex and remain poorly quantified (e.g., Sillitoe [2010] for a recent review). Clearly, two steps are required: (1) magmas need to be efficiently purged of their metal contents by the MVP, and (2) the metal-enriched MVP needs to travel through the magma reservoir in an efficient way. There is, therefore, a competition between how long the MVP remains in contact with the magma (metals enrichment dictated by diffusion) and how fast the MVP can be transported upward (advection). This competition can be best explored using the dimensionless Péclet number.

[6] Previous modeling on metal extraction from magma [Candela, 1986, 1989a, 1989b, 1991; Cline and Bodnar, 1991; Simon et al., 2008] have mainly focused on the first stage described above. The problem was considered as static (no gas transfer) and calculated the evolution of the metal concentrations in the MVP in a closed-system, crystallizing magma body. In the present paper, we focus on the role of transport dynamics, assessing the relative importance and consequence of the two stages delineated above by taking into account both the diffusion of elements as well as their transport by advection in a magma reservoir that grows from periodic recharge and reaches a crystalline mush state.

## 2. Previous Work

### 2.1. MVP Transport in Magma Reservoirs

[7] Owing to the MVP's buoyancy in the shallow crust ( $\rho_{\text{fluid}} \sim 4\text{--}5$  times lower than  $\rho_{\text{magma}}$  [Lemmon et al., 2003]), a large amount of gravitational potential energy is available for the fluids to ascend. However, the MVP transport mechanism and efficiency remains poorly understood. This section provides a summary of previous work on this topic, and describes how we build upon it to describe volatile transport and metal extraction across a range of dynamic regimes.

**Table 1.** List of Symbols

|                      | Description  |
|----------------------|--|
| $\delta$             | average pore size in the mush  |
| $\varepsilon_i$      | enrichment factor ( $=C_i^g/C_i^m$ )   |
| $\varepsilon_{ij}$   | ratio of $\varepsilon_i/\varepsilon_j$                                       |
| $\phi$               | porosity   |
| $\mu$                | dynamic viscosity  |
| $\rho_j, \Delta\rho$ | density of phase $j$ and density difference                                  |
| $\Psi$               | loading ability of the intrusion (injection of MVP)                          |
| $A$                  | mush-intrusion surface area  |
| $C_i^m$              | concentration of element $i$ in the melt                                     |
| $C_i^g$              | concentration of element $i$ in the MVP                                      |
| $D_i$                | diffusion coefficient of element $i$ in the melt                             |
| $g$                  | acceleration due to gravity  |
| $H$                  | thickness of mush overlying the intrusion                                    |
| $K_i$                | partition coefficient between MVP and melt for element $i$                   |
| $k, k_r$             | mush permeability and relative (multiphase) permeability                     |
| $m_{H_2O}$           | solubility of water in the magma   |
| $M$                  | mass ratio between the MVP and the melt                                      |
| $\dot{M}_i$          | mass flux of element $i$ to the top of the mush                              |
| MVP                  | magmatic volatile phase  |
| Pe                   | Peclet number $= U_g(\delta - R)^2 / (MD_iH)$                                |
| $R$                  | bubble/MVP channel radius  |
| $S$                  | MVP pore volume fraction (also referred to as saturation)                    |
| $S_r$                | residual saturation = critical pore volume fraction: connected pathways form |
| $U_b$                | free ascent velocity for a bubble  |
| $U_g$                | pore MVP velocity in channel   |
| $U_g^0$              | reference pore MVP velocity  |

[8] The separation of buoyant, exsolved volatiles as independent bubbles or bubble plumes from magmas has been invoked as the main process to extract volatiles from the magma chamber [e.g., *Candela, 1991; Linde et al., 1994; Cardoso and Woods, 1999; Phillips and Woods, 2002; Costa et al., 2006; Ruprecht et al., 2008*]. However, bubble rise (as single bubble or trains of bubbles) in viscous magmas is sluggish. For isolated bubbles, their steady state separation velocities can be approximated by Stokes ascent velocity

$$U_b = \frac{\Delta\rho g R^2}{3\mu_m}, \quad (1)$$

where  $\Delta\rho$  is the density contrast between the bubble and the surrounding melt,  $R$  the radius of the bubble and  $\mu_m$  the dynamic viscosity of the surrounding melt ( $\sim 10^4 - 10^5$  Pa s in silicic magmas). The list of symbols can be found in Table 1. Because melt viscosity dominantly controls the resistance to the ascent of the bubble, they reach ascent velocities of less than one m/year for mm-sized bubbles in a rhyolitic melt. Having larger bubbles or bubble plumes (containing many closed-packed bubbles), can increase the ascent velocity [*Ruprecht et al., 2008*], but the presence of hindering factors (such crystals or neighboring bubbles) will likely slow down the MVP ascent in natural systems.

[9] If connected volatile pathways can form as the amount of exsolved MVP increase, the ascent velocities of exsolved volatiles will increase by orders of magnitude as the resistance to the ascent is controlled by the low viscosity fluid rather than the high viscosity silicate melt. Such connected channels are unlikely to form in low crystallinity environments, because they tend to be disrupted by convection currents and are susceptible to perturbations (e.g., variation of cross section) that would lead to capillary instabilities [*Zhang and Lister, 1999; Sierou and Lister, 2003; Parmigiani et al., 2011*]. In contrast, a high-crystallinity environment (e.g., a mush state), can promote the development of stable volatile channels (and resulting much faster ascent rates of volatiles relative to individual bubble ascent rates [*Parmigiani et al., 2011*]). The reasons are the following:

[10] 1. Crystals make up much of the magma volume, concentrating the melt and exsolved MVP in the pore space.

[11] 2. The crystal framework hamper convection due to the appearance of yield strength [*Vigneresse et al., 1996; Philpotts et al., 1998; Walsh and Saar, 2008; Karlstrom et al., 2012*].

[12] 3. Crystallization leads to increased volatile concentrations in the residual melt (second boiling [*Burnham, 1979*]).

[13] It is important to note that, high crystallinity environments are the most common state in which magmas are preserved in reservoirs due to diminished thermal gradients and latent heat buffering [*Marsh, 1981; Koyaguchi and Kaneko, 1999; Huber et al., 2009; Dufek and Bachmann, 2010*].

[14] As connected pathways only sample a limited fraction of the mush at any one time (Figure 1b), a single episode of volatile release and upward transport may not reach every part of the mush. However,

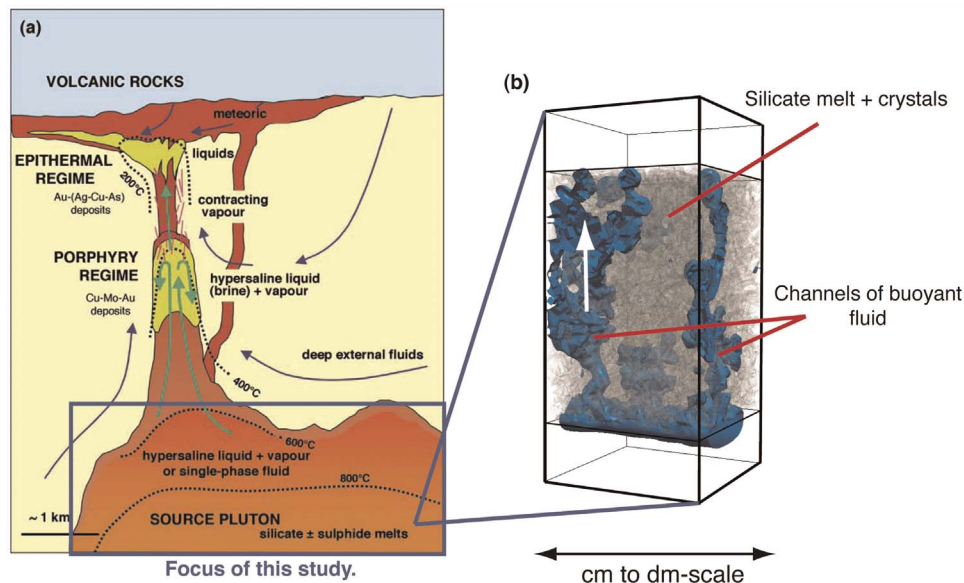


**Figure 1.** (a) Schematic diagram of the magmatic-hydrothermal system, illustrating the different mass transport and thermal regimes (modified from Heinrich [2005]). In this study, we focus on the dynamics of extraction and transport of magmatic fluid out of the source pluton. (b) Result of a numerical calculation of multiphase flow in porous media taken from Parmigiani et al. [2011]. The buoyant fluid is shown in blue, the crystal in light gray and the residual melt is transparent to help visualize the formation of buoyant fluid channels.

in an incrementally built system with many recharge events [Vigneresse, 2007], connected pathways can form in different areas, selected stochastically during the evolution of the magmatic system. A more detailed discussion of the formation and stability of connected channels of MVP (including the efficiency of the leaching process) is presented in section 3.

## 2.2. Previous Models of Metal Purging From Magma Reservoirs

### 2.2.1. First Stage: Partitioning of Elements Between the Melt and the MVP

[15] Candela [1986, 1989a, 1989b, 1991] and Cline and Bodnar [1991] developed models to calculate the partitioning of trace elements between the melt and the MVP after volatile exsolution in a static (isobaric) and closed-system case (increase in MVP volume fraction due uniquely to second boiling). In these models, exsolution is treated as a Rayleigh fractionation process, i.e., new increments of exsolved MVP equilibrate with the co-existing silicate melt but do not equilibrate with the MVP exsolved previously. In that context, the efficiency of removal of an element (the total fraction of a given element that goes in the MVP) can be computed as function of a

progress variable that measures the fraction of water exsolved in the system.

[16] Candela's model offers an elegant approach to quantifying the mass partitioning of elements compatible with the MVP during a closed-system exsolution process. However, it neglects time-dependent transport and, as such, it only provides an upper bound for the efficiency of removal of MVP-compatible elements during exsolution. This upper bound arises because, in Candela's model, chemical equilibrium is always reached between the melt and the MVP before the latter segregates away from the crystallizing silicate melt. It is also important to note that the assumption of Rayleigh fractionation is unlikely to be valid in a MVP-silicate melt system. In magmatic environments, Rayleigh fractionation is typically used for the crystallization of solid phases, in which chemical diffusion of elements is extremely slow [e.g., Zhang and Cherniak, 2010]. In the case of the exsolution of a MVP during second boiling, once bubbles have nucleated, volatile transfer from the melt to the volatile phase proceeds mostly by bubble growth rather than repeated nucleation events because the saturation pressure are not expected to reach the threshold for homogeneous nucleation [Hurwitz and Navon, 1994; Mangan and Sisson, 2000]. As a consequence, the homogenization of trace elements within the MVP

(by diffusion and convection) will be rapid. Moreover, as discussed previously, the advection of the MVP through a crystal-rich silicic magma is slow unless the MVP forms connected pathways.

[17] In the light of the previous argument, we argue that equilibrium fractionation of trace elements between the fluid and the melt during exsolution may be more appropriate to compute the enrichment of the MVP in compatible trace elements prior to the formation of connected MVP pathways. That is, when the MVP takes the form of isolated bubbles, it is in equilibrium with each parcel of melt it encounters and is transport- rather than diffusion-limited. This has important consequences from the trace element evolution in the magmas and MVP. For example, after 20% exsolution, an element with a  $D^{\text{fluid/melt}}$  of 60 (e.g., Cu) would have a  $C_{\text{fluid}}/C_0 \sim 40,000$  larger in the equilibrium than in the fractional case. Invoking an equilibrium process retains more compatible elements in the melt as exsolution proceeds, hence reducing the efficiency of the purging effect predicted by Candela's models.

### 2.2.2. Second Stage: Transport of MVP out of the Reservoir

[18] Although not included in the models of metal concentrations in the MVP phase, Candela [1986, 1989a, 1991] discussed the transport of the MVP in a crystallizing magma chamber and defined the concept of "spanning clusters" (derived from percolation theory) that defines the formation of a connected MVP phase across the magma body. Using two-phase percolation theory, Candela's model suggested that these spanning clusters form as the volume fraction of MVP approaches 30 vol% of the magma.

[19] Although we follow a similar concept, there are two major differences between the concept of spanning clusters introduced by Candela [1986, 1989a, 1991] and the formation of capillary channels above a residual saturation threshold  $S_r$  that we consider in the study. First, capillary channels are predicted from multiphase dynamics, whereas spanning clusters are purely a geometrical construct. In standard percolation theory, the distribution of MVP is random and, on average, clusters are expected to form isotropically, whereas the MVP transport is not static and buoyancy forces introduce anisotropy due to gravity. This important difference has a tendency to decrease the critical volume fraction required for connectivity for  $S_r$ . Second, the threshold at which spanning clusters are expected to form, according to Candela's model, depends only on the volume fraction of MVP (about 30%). In

multiphase flows in porous media, the connectivity of MVP clusters actually depends on the volume fraction of the pore-space occupied by the MVP. The correct "percolation" criterion is therefore controlled by the relative abundances of the three phases (melt-crystals-MVP) and, as such, it depends explicitly on the crystallinity in the magma. Fixing  $S_r$  to a value of about 20%, as is generally done for multiphase flows [Bear, 1972], yields a critical volume fraction of MVP of 10% and 6% for crystallinities of respectively 50 and 70%.

### 2.2.3. Kinetic Versus Equilibrium Chemical Exchanges

[20] As transport is not taken into consideration in the mathematical model presented by Candela [1986, 1989a, 1991], chemical equilibrium is assumed between new increments of MVP and the melt (Rayleigh distillation process). In other words, the time allowed for chemical equilibration between the two phases is longer than the time required for the studied trace element to diffuse from the melt to the MVP. Using such an assumption, Candela [1986, 1989a, 1991] showed that the knowledge of the bulk partition coefficient of the trace element and the ratio of dissolved water at saturation to the initial dissolved water content control the efficiency of removal of the element out of the magma.

[21] Chemical equilibrium between the melt and the MVP requires that, between the time for the growth of a new increment of MVP and its transport out of the system, diffusion of trace elements in the melt is rapid enough to erase chemical potential gradients. Such an assumption is likely to be fulfilled for fast diffusing species at low MVP volume fraction, when advection is extremely slow. However, as the MVP pore volume fraction approaches the threshold where it forms connected capillary channels (residual saturation  $S_r$ , set at  $\sim 20$  vol% of remaining pore space), advective transport becomes important and chemical equilibrium is limited by the competition between diffusion to and advection of the MVP. Hence, the use of equilibrium partition coefficients during the diffusion-limited exchange of metals between the melt and the MVP is no longer valid in a highly crystalline magma reservoir containing MVP channels, and the mass balance between the melt and the MVP needs to be computed with a kinetic model.

[22] Assuming that MVP advection is non-negligible, the competition between diffusion and transport controls the metal enrichment of the MVP. For chemical exchange of trace elements to occur during

the ascent of the MVP in the overlying crystal-mush, a chemical disequilibrium is required between the ascending MVP and the residual melt in the mush. We have isolated three conditions under which the MVP exsolved from a magma recharge has the potential to gather more metals with the overlying crystal-rich reservoir as it travels upwards:

[23] 1. A difference in composition between the recharge and the mature mush (assumed to be dacitic). For reasons discussed in section 3 below, this scenario should be considered as second order and is not studied here.

[24] 2. The magma recharge, after exsolution, is chemically identical to the overlying mush, but the diffusion of metals from the melt to the MVP during exsolution was not fast enough to prevent disequilibrium. In that context, once the MVP reaches the critical pore volume fraction that allows for an efficient transport, (above the residual saturation threshold  $S_r$ ), it ascends through the mush while being in disequilibrium with the host melt.

[25] 3. The formation of connected pathways and the initiation of the fast transport of MVP in the recharge occur at a crystallinity that is below the crystallinity of the overlying mush. Trace elements that are incompatible with crystalline phases are therefore enriched in the residual melt of the mush compared to the MVP that was formerly in chemical equilibrium with the less mature melt of the recharge. This disequilibrium condition can explain the uptake of trace elements by the MVP during transport for incompatible elements only.

### 3. Proposed Model

[26] We assume a dynamical scenario where a mature crystal-rich mush ( $\geq 50\%$  vol% crystals) grows from repeated recharges of magma with a similar bulk composition ( $\sim$  dacitic as a proxy for the average upper continental crust [e.g., *Rudnick and Gao, 2003*]), but higher temperature and lower crystallinity (see review by *Lipman [2007]* for incremental growth of large reservoirs). More mafic magmas (basalts, andesites) can periodically be recharged as well, but (1) their relative small volume in these upper crustal mushes, and (2) their metal contents that are typically similar to or lower than dacites, make magma bulk composition unlikely to affect the model significantly.

[27] As these recharge batches equilibrate thermally with the overlying mush column, volatiles are exsolved as a result of second boiling. The

buoyant low-viscosity MVP is expected to form capillary fingers in the mush due to Saffman-Taylor instabilities ([*Saffman and Taylor, 1958*] a full discussion of the formation and stability of capillary fingering instabilities derived from pore-scale calculations is beyond the scope of this paper, but the reader is referred to *Parmigiani et al. [2011]* for more details on this process). As a consequence of this fingering instability, the MVP will be distributed heterogeneously and reach locally a high pore volume fraction  $S$  that can vastly exceed the residual saturation  $S_r$  threshold of  $\sim 0.2$  (20 vol% bubble; see Figure 1b), generating connected pathways. The existence and spatial density of these fingers depends on the mass flux of aqueous fluids released by the underplating recharge and on the permeability of the mush [*Parmigiani et al., 2011*] and will vary through time. We focus on the diffusion of metals from the silicate melt to the exsolved volatile phase moving upward in connected pathways to the top of the magmatic column (Figure 2).

[28] Considering an average melt-aqueous solution diffusion path length of  $\delta - R$ , where  $\delta$  is a measure of the average pore size, and  $R$  of the average radius of the aqueous fluid pathway (see Figure 2), the simplified 1-D mass conservation equations for the element  $i$  in the aqueous and melt phases are

$$\begin{aligned} \frac{\partial C_i^g(z, t)}{\partial t} + U_g \frac{\partial C_i^g(z, t)}{\partial z} - \frac{MD_i}{(\delta - R)^2} (C_i^m - K_i C_i^g) &= 0 \\ \frac{\partial C_i^m(z, t)}{\partial t} + \frac{D_i}{(\delta - R)^2} (C_i^m - K_i C_i^g) &= 0, \end{aligned} \quad (2)$$

where  $C_i^x$  is the concentration of element  $i$  in the phase  $x$  ( $g = \text{gas}$ ,  $m = \text{melt}$ ),  $U_g$  is the average pore fluid velocity for the MVP,  $D_i$  and  $K_i$ , respectively, the diffusion coefficient and the MVP-silicate melt partition coefficient for the element  $i$ .  $M$  is the mass ratio of the two fluids ( $\rho_m/\rho_g$ )( $\delta/R - 1$ ), where  $\rho_m$  and  $\rho_g$  are the density of the melt and aqueous fluid, respectively.

[29] In the set of equation (2), we neglected the vertical component of diffusion because of the elongated geometry of connected fluid pathways (i.e., the pore size  $\ll$  than the mush thickness over which the solution is transported). For all calculations, we assumed that the pore size  $\delta$  is on the scale of a few crystal lengths (mm to cm) and  $R$  is calculated by imposing a given pore volume fraction of exsolved fluid  $S$  (see next sections). The mass conservation equations for each fluid phase are coupled and we solve them numerically using an implicit finite difference method. The grid spacing and time stepping have been varied to ensure convergence of

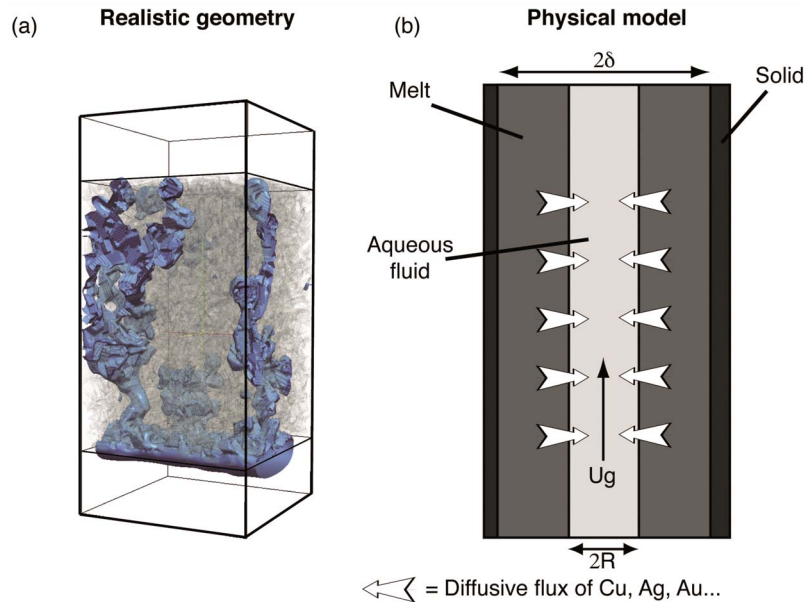


**Figure 2.** Schematic illustration of the physical model for the metal transport in the crystal mush.

the results over the range of calculations we conducted. The initial concentration is normalized so as to be equal to 0 in the aqueous fluid and 1 in the melt for simplicity (the model is designed for elements that fractionate into the fluid phase)

$$C_i^x(z, t) = \frac{C_i^x(z, t) - C_i^g(z = 0, t = 0)}{C_i^m(z = 0, t = 0) - C_i^g(z = 0, t = 0)}. \quad (3)$$

In the equation above,  $x$  is the phase ( $m$  or  $g$ ) and  $C'$  is the actual concentration (un-normalized). We decided to use this normalization to keep the calculations as generic as possible. However, we emphasize that this choice does not mean that we assume the concentration of element  $i$  in the MVP to be zero as it enters the overlying mush, rather that we focus our attention to the chemical exchange between the MVP and a more evolved melt in the overlying mush as a secondary enrichment process. In that sense, the amount of enrichment that we compute here focuses on the scavenging of metals from an incompletely depleted mush. Assuming that the enrichment of the MVP with respect to the melt in the magma recharge after exsolution (before the transport in the overlying mush) is given by

$$\varepsilon_i^0 = \frac{C_i^g(\text{recharge})}{C_i^m(\text{recharge})} \frac{C_i^m(\text{recharge})}{C_i^m(z = 0, t = 0)}, \quad (4)$$

where the first term in the right-hand side is the partitioning in the recharge after exsolution (generally assumed to be equal to the MVP-melt partition coefficient) and the second term introduces the differences in melt composition between the recharge

after exsolution and the more evolved residual melt in the mush. If the latter term is equal to unity, i.e., same concentration of trace element  $i$  in the recharge melt and in the mush melt, then the chemical exchange only occurs during exsolution. This end-member case corresponds to the model of *Candela* [1986, 1989a, 1991] and *Cline and Bodnar* [1991]. On the other hand, if the second fraction on the right-hand side of equation (4) is greater than unity (e.g.,  $i$  corresponds to an incompatible element and the melt in the mush is more evolved), the system of equation (2) will allow us to calculate the kinetics of the enrichment of element  $i$  in the MVP as it rises through the magmatic column.

[30] A key assumption of the model is that connected pathways of MVP can form in these crystal-rich mushes (we use here a residual saturation threshold  $S_r = 0.2$ ). Using the MELTS software [Ghiorso and Sack, 1995] to compute the relative proportion of exsolved  $\text{H}_2\text{O}$ , melt and crystals in a dacitic magma with initial water content from 4 to 7 wt%, we show that 50–60 vol% crystallization of such volatile-rich dacitic magma at about 2 kbars can lead to the development of MVP pore volume fractions equivalent to  $S_r$ . These MELTS calculations do not take into account the effect of  $\text{CO}_2$ , and therefore are minimum estimates of the bubble vol.% fraction in the melt as  $\text{CO}_2$  has a low solubility in silicate melts, and will readily add mass to the exsolved phase. Hence, these thermodynamic calculations indicate that, in a closed-system, the volume (at 2 kbars) of MVP exsolved in magmas with 4–7 wt%  $\text{H}_2\text{O}$  is

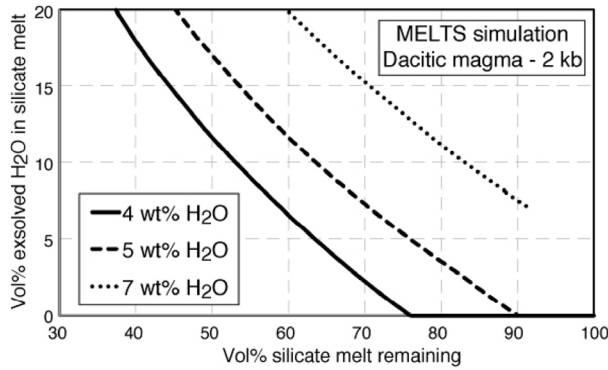
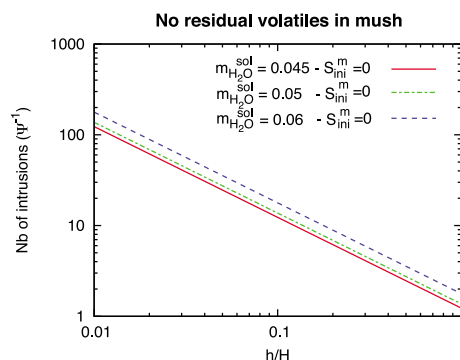


**Figure 3.** Vol.% exsolved H<sub>2</sub>O in melt with respect to amount of silicate melt remaining in the system for dacitic magmas at 2 kb (calculated from MELTS [Ghiorso and Sack [1995]). We use a range of initial water contents (from 4 to 7 wt.%), which is typical of most magmas in subduction zones.

great enough to form percolating pathways through the mush when these silicic magmas reach a crystallinity of about 40–60% (Figure 3). However, if volatile losses were to become important during the crystallization of the magma (open-system behavior with respect to the MVP), then outgassing from underlying recharge (“gas replenishment”) become necessary to build these volatile channels through the mush.

[31] If magmas experience open-system degassing during some periods of their storage in the shallow crust, we need to quantify the number of recharge events that are necessary to provide exsolved volatiles to the overlying magma column in order to build stable and percolating MVP channels. The mass of volatile exsolved by the newly intruded magma per unit surface area during its equilibration with the mush is given by

$$M_{H_2O} = \rho_m h [m_{H_2O} \phi^0 - m_{H_2O}^{sol} \phi (1 - S)], \quad (5)$$



where  $S$  is the pore volume fraction of MVP,  $\rho_m$  is the density of magma,  $h$  is the thickness of the recharge,  $m_{H_2O}$  is the initial water content of the magma (in weight percent),  $\phi^0$  the melt fraction (1 – crystallinity) when the recharge is emplaced,  $m_{H_2O}^{sol}$  the solubility of water in the magma (here taken as a dacite at 2 kbar and about 750°C). The crystallization of the recharge magma leads to a change in melt fraction from  $\phi^0$  to  $\phi$  and the exsolution of a volume fraction  $\phi S$  of volatiles. Similarly, one can compute the minimum mass of MVP to add to the overlying mush of thickness  $H$  so that the saturation level  $S_r$  ( $\sim 20$  vol% bubble) is reached, starting from a given saturation  $S_{ini}$  lower than  $S_r$ .

$$M_{H_2O}^m = \rho_{H_2O} H \phi_m (S_r - S_{ini}), \quad (6)$$

where  $\rho_{H_2O}$  is the average density of exsolved water in the mush (taken here for simplicity to be about 600 kg/m<sup>3</sup>), and  $\phi_m$  is the melt+MVP volume fraction (1 – crystallinity) in the mush. The sudden change in transport efficiency for the MVP above and below  $S_r$  suggests that  $S_{ini}$  may be only a few volume percent below  $S_r$ . Defining the MVP loading ability of a new recharge by the ratio  $\Psi = M_{H_2O} / M_{H_2O}^m$ ,

$$\Psi = \frac{\rho_m h [m_{H_2O} \phi^0 - m_{H_2O}^{sol} \phi (1 - S)]}{\rho_{H_2O} H \phi_m (S_r - S_{ini})}, \quad (7)$$

$\Psi^{-1}$  provides an estimate for the number of recharge events of thickness  $h$  that are required to load the overlying mush in MVP so that percolating paths are formed. Figure 4 shows how the number of recharge is affected by (1) initial water content of the newly intruded magma (Figure 4, left) and (2) the trapped saturation of MVP in the mush prior to the new intrusion  $S_{ini}$  (Figure 4, right).

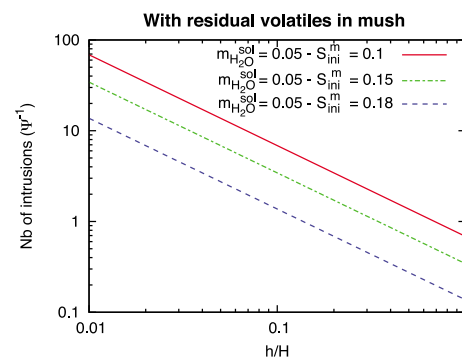


**Figure 4.** Dependence of the number of intrusions of thickness  $h$  required to load an overlying mush with enough exsolved volatiles to reach the residual saturation threshold  $S_r$ . More details in the text.

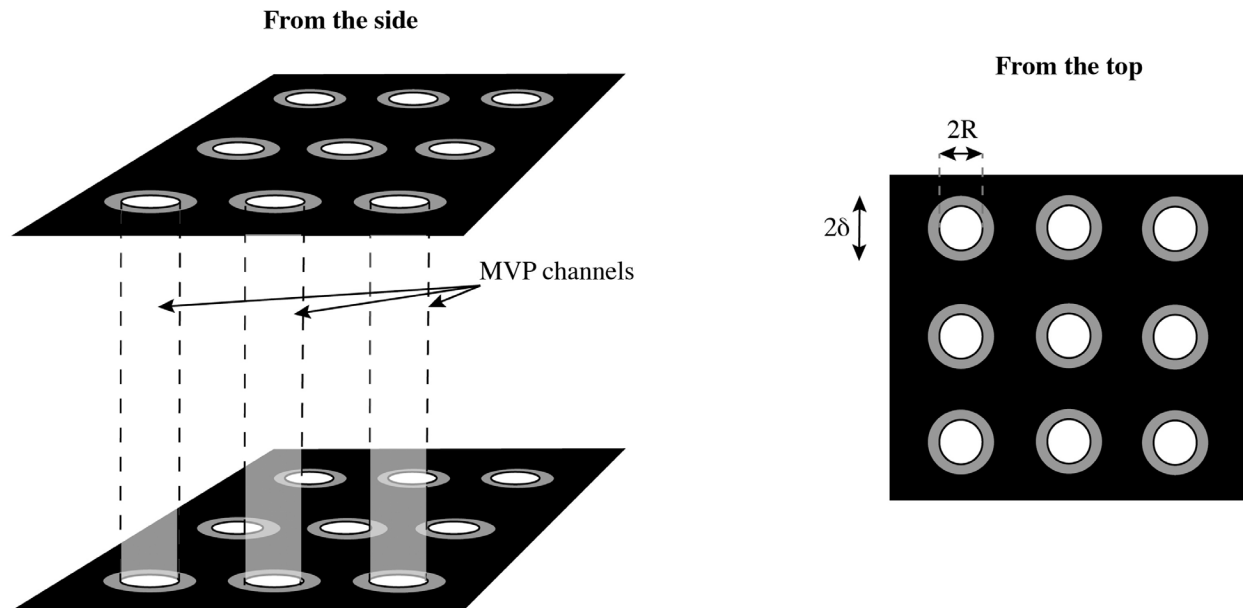


**Figure 5.** Schematic depiction of the calculation for  $F_m$ . See text for more details.

[32] Even if the magma reservoir behaves as an open-system with respect to its bubble content (outgassing), only a few small recharge events are necessary to load the mush in MVP above  $S_r$  again (Figure 4). From the MELTS calculations described above we show that second boiling of dacitic magmas at 2 kbars (for water content initially greater or equal to 5 wt%) to a crystallinity approaching 50–60% is enough to exsolve a volume of volatiles comparable to what would be required to form percolating MVP pathways. A small amount of gas can be lost as fluid pathways are open, but as soon as the pathways are disrupted, outgassing essentially stops and allows for a high volume fraction of trapped MVP in the magma reservoirs ( $S_{ini}$ ). Hence, a dacitic recharge with 5 wt%  $H_2O$  10 times smaller than the mush would be enough to allow MVP pathways to be re-established if residual saturation did not decrease below 18 vol% (Figure 4).

[33] If connected pathways of MVP are likely to form regularly during the incremental growth of mature crystal-rich mushes, one can question the efficiency of each outgassing event in terms of metals extraction out of the melt. More precisely, what is the fraction of residual melt in the mush that is located within a distance  $\delta - R$  of MVP channels. We assume that the radius  $R$  of each of these MVP channels is controlled by the geometry of the pore-space, which is in term governed by the average crystal-size. For simplicity, the spacing between

channels will be assumed constant (see Figure 5). The number of channels crossing a surface area  $A$  in the mush is given by

$$N = \frac{A\phi_m S_r}{\pi R^2}. \quad (8)$$

The fraction of the melt that lies within a distance smaller or equal to  $\delta - R$  from an MVP channel is therefore

$$F_m = \frac{(\delta^2 - R^2)}{R^2} \frac{S_r}{1 - S_r}. \quad (9)$$

Using  $\delta = 2R$ , we get that the fraction of the melt in the mush that lies within a distance  $\delta - R$  from a percolating MVP channel is 75%, versus about 30% for  $\delta = 1.5R$ . Using the simple geometrical model of annular flows, a rough upper bound for the size of the annuli  $\delta < 2.23R$  can be determined by imposing that the pore volume fraction of MVP in these annuli is greater than  $S_r$ . In any case, this shows that the leaching process in the mush can be very efficient, especially when considering that the position of percolating pathways can change stochastically in successive outgassing events.

[34] A major difference between the transport model of Candela and ours is that the high crystallinity region is not confined here to the outer edge of the magma reservoir (in “sidewall solidification fronts”

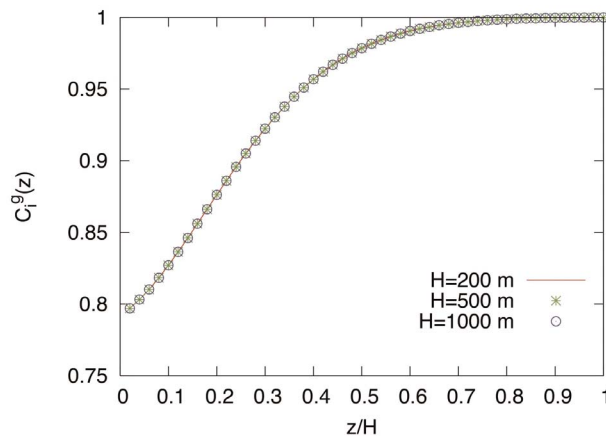


**Figure 6.** Comparison of the self-similarity of the solution to equation (2). Here  $Pe$  is fixed to 0.21, the thickness of the mush is varied from 200 to 1000 m (the melt diffusivity  $D_i$  was used to compensate for the change in mush thickness and keep  $Pe$  fixed). The concentration in the MVP as it enters the overlying mush is set to  $\varepsilon_i^0 = 75$ .

[e.g., *McBirney et al.*, 1985; *Nilson et al.*, 1985; *Marsh*, 1996], but that the crystallinity is assumed to be more homogeneous throughout the magma body [*Huber et al.*, 2009]. Field observations [*Bachmann and Bergantz*, 2004], fluid dynamics calculations [*Bergantz and Ni*, 1999; *Dufek and Bachmann*, 2010] and thermal considerations [*Huber et al.*, 2009] suggest that *sharp* sidewall solidification fronts nucleating on the edges and converging toward the center of the intrusion, tend to be rare in magma reservoirs. The main reasons for the paucity of solidifications fronts in magmatic systems are: (1) a substantial fraction of the crystals can be entrained in crystal-laden plumes, continuously destroying solidification fronts growing on the sides of magma chambers (particularly in sill-like reservoirs [e.g., *de Silva and Wolff*, 1995]) and (2) heat loss from the reservoir tends to be buffered by latent heat at high crystallinity, particularly in silicic magmas, leading to a homogenization of crystallinity through time [*Huber et al.*, 2009]. We therefore expect the active (melt-bearing) part of the magma reservoirs to be fairly homogeneous in crystallinity throughout (apart from potential melt-rich cupolas in the upper part of the reservoirs [*Bachmann and Bergantz*, 2004; *Hildreth*, 2004; *Bachmann and Bergantz*, 2008]). Most of the magma reservoirs (and not only volumetrically limited sidewall solidification fronts) will therefore participate in the formation of gas channels, which

will favor the chemical exchanges between the melt and the MVP during the transport.

## 4. Results

[35] Our 1-D model admits a unique dimensionless number that characterizes the efficiency of the aqueous fluid to extract and transport elements up through the mush, the Péclet number ( $Pe$ ).  $Pe$  quantifies the ratio of advective to diffusive flux of element  $i$ . Balancing the advective with the diffusive transport terms in equation (2), we define  $Pe = U_g(\delta - R)^2/(MD_iH)$ , where  $H$  is the thickness of the overlying mush. We, therefore, expect the solution of the set of equation (2) to be self-similar, i.e., that normalized concentration profiles obtained for a different set of parameters will be identical for a fixed value of  $Pe$  and a given time. Our numerical calculations confirmed the self-similar nature of the solution (see Figure 6), which compares the normalized concentration profiles in the melt and exsolved fluid in mushes of different thicknesses.

[36] This self-similar behavior has profound implications; it requires that, as long as the Péclet number values (as defined above) are identical, the concentration ratio of an element between the MVP and the melt remains the same. In essence, within the assumptions of this model, the departure from the equilibrium partitioning between the melt and the MVP at the top of the magmatic column depends only on the Péclet number and time. At low Péclet number, the system will tend to thermodynamic equilibrium and the concentration ratio of a given element will approach the value of the partition coefficient. However, at high Péclet number, the kinetics of this system will lead to significant divergence from the equilibrium partitioning between the melt and the MVP except for very long times (when equilibrium is reached).

[37] Numerical simulations using the set of equation (2) show that the composition and mass flux of precious metals to the hydrothermal system is strongly controlled by the competition between diffusion from the magmatic melt to the magmatic fluid, and the buoyant advective transport of the latter. First, we observe that the time to reach steady state decreases with decreasing  $Pe$ . The characteristic timescale is given by  $\tau \sim (\delta - R)^2/(MD_i)$  (middle row, Figure 7). Once the steady state is established, regardless of the value of  $Pe$ , the ratio of the MVP to the melt concentration in element  $i$  at the top of the mush (height  $H$ ) is equal to the

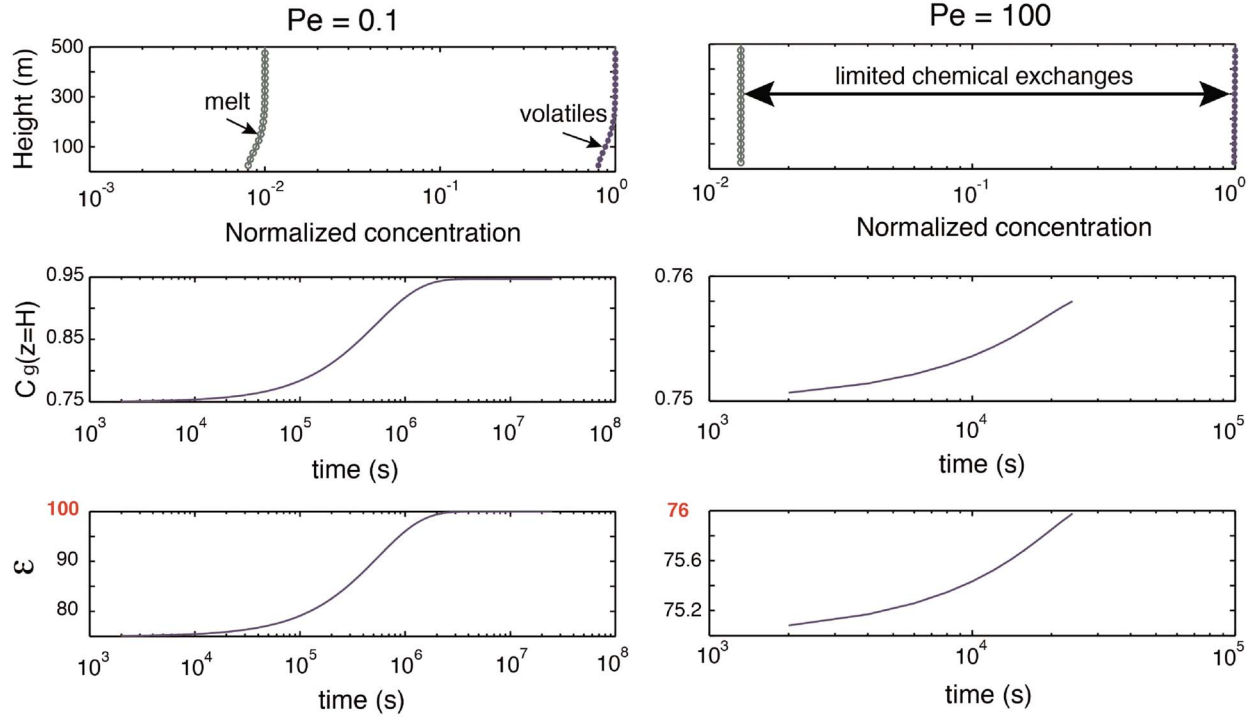


**Figure 7.** Comparison of model calculations with different  $Pe$  (different ratios of advective to diffusive element flux). The top row shows the normalized concentration profiles in both melt (green) and MVP (blue). The initial concentration is set to 0 in the MVP and 1 in the melt for simplicity. The middle and bottom rows show the temporal evolution of the normalized concentration in the MVP and the enrichment factor at the top of the mush column respectively ( $H = 500$  m for those calculations, and the partition coefficient for element  $i$  between fluid and melt  $K_i = 100$ ). In these two calculations, the initial disequilibrium between the residual melt in the mush and the penetrating MVP is  $\varepsilon^0 = 75$ . The calculation time corresponds in both cases to the time it takes a parcel of MVP to ascend through the mush (shorter for higher  $Pe$ ).

partition coefficient. In order to be self-consistent in the characterization of the melt-MVP chemical exchanges, we study the concentration ratio of an element between the MVP and the melt at the top of the mush  $\varepsilon_i$  after a time  $t^* = H/U_g$  that corresponds to the time for a parcel of MVP to rise through the overlying mush

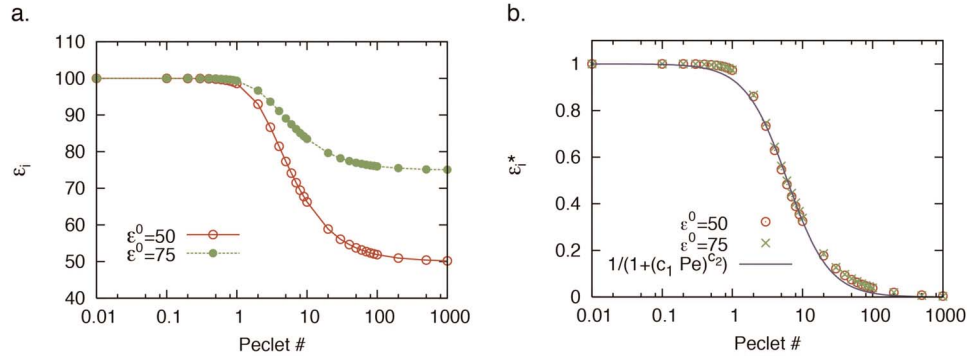
$$\varepsilon_i = \frac{C_i^g(z = top, t^*)}{C_i^m(z = top, t^*)}. \quad (10)$$

Figure 7 shows that  $\varepsilon_i$  is strongly controlled by  $Pe$ . For the low  $Pe$  ( $< 0.1$ ) case shown here, the enrichment factor reaches the maximum value ( $=K_i$ , the partition coefficient) because the diffusive process is fast enough for the two phases to reach equilibrium. However, when  $Pe \sim \geq 1$ , the equilibrium assumption grossly overestimates the actual steady state enrichment factor (bottom row, Figure 7).

[38] We conducted a series of calculations to highlight the dependence of the enrichment factor

(Figure 8a) on  $Pe$  and on the disequilibrium between the MVP and the residual melt in the mush  $\varepsilon_i^0$ . At  $Pe < 1$ , the enrichment factor saturates to the partition coefficient value (here arbitrarily fixed at 100) and the concentration of element  $i$  in the aqueous fluid is maximal. As  $Pe$  increases above unity, i.e., when the advective transport balances or slightly exceeds the diffusive transport, a power law relationship emerges with an exponent of  $-1.456$  for the enrichment factor. We also observe that the choice of  $\varepsilon_i^0$  controls the lower bound of the enrichment at high Péclet number, i.e., if the advective flux is fast enough to prevent any substantial chemical exchange between the MVP and the melt, the enrichment factor  $\varepsilon_i = \varepsilon_i^0$ . The dependence of  $\varepsilon_i$  on the initial disequilibrium between the residual melt in the mush and the MVP after exsolution can be absorbed into the definition of  $\varepsilon_i$  by introducing a normalized enrichment factor

$$\varepsilon_i^* = \frac{\varepsilon_i - \varepsilon_i^0}{K_i - \varepsilon_i^0}, \quad (11)$$



**Figure 8.** (a) Normalized concentration of a given element  $i$  in the gas phase with respect to  $Pe$  and (b) enrichment factors of an element  $i$  as a function of  $Pe$ .

as demonstrated by Figure 8b. The dependence of  $\varepsilon_i^*$  on  $Pe$  can be fitted reasonably well with a single power law relationship

$$\varepsilon_i^*(Pe) = \frac{1}{1 + (0.165Pe)^{1.456}}, \quad (12)$$

or in terms of non-normalized enrichment factor

$$\varepsilon_i(Pe) = \varepsilon_i^0 - \frac{\varepsilon_i^0 - K_i}{1 + (0.165Pe)^{1.456}}.$$

## 5. Discussion

### 5.1. Enrichment Factors as Function of Volatile Flux

[39] Our model shows that  $Pe$  controls the enrichment of metals in the MVP, but as it depends on poorly constrained parameters that can vary from one magmatic system to another (e.g., the advective

flux of aqueous fluid  $U_g$  and the characteristic average diffusion distance  $\delta - R$ ),  $Pe$  is difficult to constrain precisely for a given system. A way to circumvent some of the poorly constrained parameters is to compute the enrichment factor ratio between different elements resulting from the same outgassing event. Using equation (12) and assuming for simplicity that  $\varepsilon_i^0 = 0$ , we obtain that the enrichment ratio between element  $x$  and  $y$  for  $Pe_k < 1$  ( $k = x, y$ ) converges towards

$$\varepsilon_{x-y} = \left(\frac{K_x}{K_y}\right) \left[\frac{1 + (c_1 Pe_y)^{c_2}}{1 + (c_1 Pe_x)^{c_2}}\right], \quad (13)$$

with  $c_1 = 0.165$  and  $c_2 = 1.456$ . Figure 9 illustrates the dependence of the enrichment ratio  $\varepsilon_{x-y}$  on the Péclet number values describing the transport of the two elements  $x$  and  $y$  in this particular regime. It is interesting to note that for a given couple of elements ( $x-y$ ), i.e. fixed ratio of Péclet numbers, one element can be favorably enriched relatively to

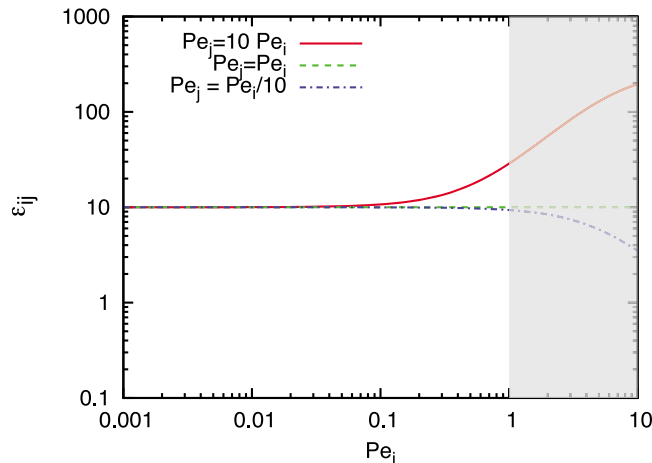


**Figure 9.** Enrichment factor ratio between element  $i$  and  $j$  as function of the Pelet number for element  $i$ . The partition coefficient ratio is fixed arbitrarily to 10 here, depending on the ratio of diffusion coefficient, the ratio can increase or decrease with  $Pe$ .

**Table 2.** Diffusivities and Partition Coefficients for Au, Cu, Cl and as Used in Figure 9<sup>a</sup>

|    | $D_i$ (m <sup>2</sup> /s) at 850°C | $K_i$ | $\delta - R$ |
|----|------------------------------------|-------|--------------|
| Au | $10^{-11}$                         | 13    | 0.1 mm       |
| Cu | $10^{-12}$                         | 63    | 0.1 mm       |
| Cl | $10^{-11.5}$                       | 8     | 0.1 mm       |
| As | $10^{-14}$                         | 2     | 0.1 mm       |

<sup>a</sup>Diffusivities from Frezzotti and Peccerillo [2004], Claußen and Rüssel [1998], von der Gönna and Rüssel [2000], and Klugel et al. [2005]. These diffusivities were all measured in silicate melts, but the melts used by Frezzotti and Peccerillo [2004] (haplogranite) had different proportion of major elements than those for Au, As, and Cu. Partition coefficients from Shinohara and Hedenquist [1997] for Cl, and Harris et al. [2003], Halter et al. [2002], Zajacz et al. [2008], and Williams et al. [1995] for Cu and Au, As. We considered partition coefficients for supercritical fluids, and did not consider the lower pressure case scenario when immiscible brine and vapor have exsolved from the supercritical fluid [e.g., Frank et al., 2011; Simon et al., 2005].

another over a range of Pe while the opposed relative enrichment can be observed over a different range of Pe (see Figure 9). From equation (13), the end-member case for  $Pe = 0$  yields ( $K_i/K_j$ ).

[40] In order to explore the enrichment behavior for four different important elements, Au, Cu, Cl and As, that all partition in favor of the MVP, we used the numerical model described by equation (2) to compute the enrichment factor ratios between elements such as Au, Cu, As, Pb and Cl (used here as a reference). The calculations were run for a duration that was defined as the time for the MVP parcel to go through a 500 meters thick overlying mush. We used different ascent velocity for the MVP so as to calculate the enrichment factor ratios for a range of

$Pe_{Cl}$  ( $10^{-3} \leq Pe_{Cl} \leq 10^3$ ). The list of partition coefficients and diffusion coefficients used for these calculations can be found in Table 2.

[41] Partition coefficient values depend on the composition of the magma, its pressure and temperature as it crystallizes. Our choice of partition coefficient values may not be optimal for a wide range of magmatic conditions. However, these calculations serve to illustrate the effect of kinetics and transport on the limitation of the chemical exchange between the MVP and the residing melt. A different choice for the set of partition coefficient will not affect the discussion and conclusion, but would rather rescale the upper bound for the enrichment factor. The effect of the competition between diffusion and transport would however remain identical.

[42] We compute the enrichment factors ratio for Au, Cu, Pb and As relative to Cl across a wide range of Péclet number (defined here with respect to Cl). In these calculations, we assumed for simplicity that  $\varepsilon_i^0 = 0$ , i.e. we focus on the enrichment of metals as the MVP ascends through the overlying magma body. When  $Pe_{Cl} \ll 1$ , the enrichment ratios converge to the ratios of the equilibrium partition coefficients for each couple of elements (region 1 in Figure 10). As the advective flux and  $Pe_{Cl}$  increases, the element with the smaller diffusivity (here As) first departs from the equilibrium partition coefficient enrichment (region 2), while Au and Cu (the two highest diffusivities) require a faster advective transport to diverge from equilibrium (region 3). The same exact features would have been measured

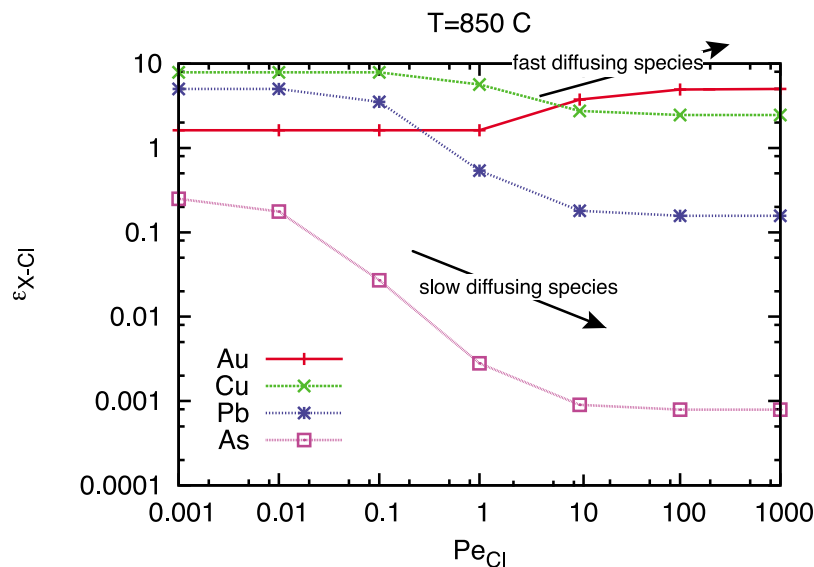


**Figure 10.** Enrichment factor for Au, Cu, Cl and As using four different pore MVP velocities. The parameters used for these calculations are listed in Table 1.

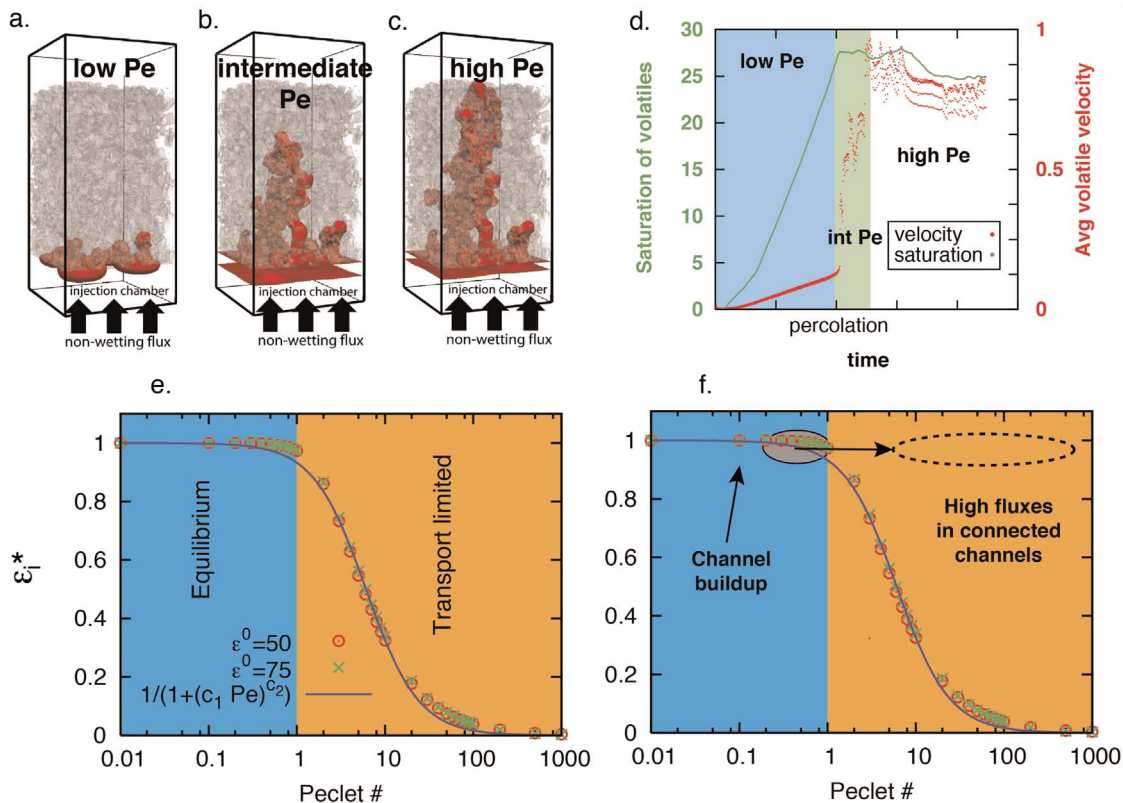


**Figure 11.** Conceptual model of melt-volatile partitioning in the mush. (a–c) These figures show three-dimensional multiphase flow calculations in a porous medium [from *Parmigiani et al.*, 2011] and illustrate the growth of capillary channels of invading fluid (here the MVP) until percolation through the system. (d) This figure shows the corresponding temporal evolution of the pore-volume fraction and discharge of invading MVP. One can easily notice the sudden increase in discharge once percolating pathways are formed (above the residual saturation threshold, here at about 25%). (e) This figure shows a breakup of Figure 8 in terms of dynamical regimes for the chemical exchanges between the melt and the volatile phase. (f) This figure illustrates the two-step model discussed in the text, whereby low Pe and efficient extraction is achieved during the build-up of the MVP channels through the mush followed by a rapid transport out of the magma body once percolating pathways have formed.

for any choice  $0 < \epsilon_i^0 < 1$ , but with a different amplitude in terms of  $\epsilon_{x-y}$  values. We stress that acquiring concentrations and partition coefficients of low concentration elements in natural samples is very challenging, and that the data have significant (albeit poorly constrained) errors associated to it. For example, the effect of different composition, T-P-fO<sub>2</sub> and “speciation” type of complex diffusing in the melt phase on the partition coefficients is poorly known [e.g., *Williams et al.*, 1995; *Candela*, 1997; *Heinrich*, 2005].

## 5.2. Importance of Péclet Number for the Extraction of Metals and Volatile Elements out of Crystal-Rich Magma Bodies

[43] In the previous sections, we discussed the importance of low Pe to ensure a near optimal

chemical exchange between the melt and the MVP (equilibrium partitioning) and pointed the limitations in terms of mass transport associated with high Pe outgassing. Here, we discuss a conceptual model that combines a low Pe stage during the build-up of capillary MVP channels in the magma body, followed by a high Pe stage of rapid outgassing once percolating pathways are formed. The latter stage allows for a rapid delivery of metals (and other elements partitioning to the MVP) out of the system. The formation of capillary channels is long compared to the time it takes volatiles to advect through the mush, hence giving rise to a third stage of intermediate Pe number values (Figures 11b and 11d). The limitations on the development of these channels are the high viscosity of the ambient fluid (highly viscous silicic melt), and the build-up of capillary pressures large enough to ensure the invasion of the

smallest pore-throats along the pathway. The advective velocity for the MVP can increase by several orders of magnitude once percolating channels are finally formed. Figures 11a–11d show an example calculation using the lattice Boltzmann method for multiphase fluids (MVP in red, melt transparent in Figures 11a–11c) and the pore-volume fraction of MVP ( $S$ ) and the average discharge of MVP ( $U_g \phi S$ ) as function of dimensionless time. One clearly sees the abrupt increase in discharge once percolating pathways are build, even though the relative increase in discharge reported from these calculation grossly underestimates what we predict for magmatic environment, because these calculations used a viscosity ratio (MVP/melt) of 1 [Parmigiani *et al.*, 2011].

[44] In summary, we envision a build-up stage of capillary channels with slow advective velocities of MVP (low Pe). From our calculations, this stage should lead to enrichment factors close to or equal to equilibrium (partition coefficients) depending on the chemical diffusivity of the element considered. The trapped MVP becomes therefore highly enriched in elements that partition from the melt to the volatile phase but stalls in the magma body until growing capillary channels percolate through the mush. Obviously, the higher the concentration of the element in the melt, the higher it will be in the MVP. Hence, as most metals are largely incompatible with igneous assemblages in silicic upper crustal magmas, the more crystallization occurred, the higher the enrichment in the melt and in the MVP (except for really high crystallinities, see Figure 2 of *Candela* [1989b] for Cu).

[45] Once percolation is achieved, rapid outgassing is possible (little chemical exchange between the melt and the already enriched MVP), extracting the enriched MVP out of the magma body and bringing it into the overlying hydrothermal system (see Figures 11e–11f). The pressure build-up at the top of the mush once the mass transport of MVP becomes important can be associated with the sudden release of MVP to the overlying hydrothermal system [see *Burnham*, 1985].

[46] For an optimal extraction of the metals, both stages need to be efficient. Hence, the magmatic conditions need to be:

[47] 1. Not too water-poor, nor too deep: this would limit the ability of the mush to transport the fluid in the upper part of the system as  $S_r$  would be attained late, once the permeability of the system has dropped significantly.

[48] 2. Not too water-rich or too shallow: this would allow rapid built-up of exsolved gas, leading to excessing volcanic venting, and outgassing at low crystallinity, when concentrations of metals in fluids and MVP are low.

[49] As magmatic systems will not strike the right balance to reach these optimal conditions in each case, large amounts of ore deposits will only occur in some intrusions, leaving all others nearly barren.

## 6. Conclusion

[50] The provenance of metals in porphyry and epithermal deposits is commonly attributed to extraction from magma bodies. The ten to thousand-fold enrichment observed in fluid inclusions [*Halter et al.*, 2002; *Harris et al.*, 2003] highlights the importance of exsolved MVPs in the transport of these metals from the original magma to the deposit. There has been considerable work over the last two decades toward unraveling the complex thermodynamics that control the transport efficiency of metals in solution at shallow depths and the factors that affect their solubility in the hydrothermal system. However, the processes that govern the extraction of these metals from the shallow magma body remain elusive.

[51] In this study, we propose a model whereby metals are leached out of a mature (i.e., crystal-rich) silicic magma body during the ascent of buoyant fluids (MVP) exsolved from recharge magma bodies. This model is complementary to previous models of metal enrichment during MVP exsolution [*Candela*, 1986, 1989a, 1991; *Cline and Bodnar*, 1991] in the sense that it focuses on the MVP enrichment in metals after exsolution, while the MVP is transported through the magma column of the magmatic system. Our model does not assume chemical equilibrium between the residual melt and the MVP and therefore allows us to study the effect of kinetics (diffusion) and transport (advection) on the efficiency of metal extraction. Using a 1-D model that includes diffusion and differential ascent rate for the MVP, we find that the relative enrichment between the MVP and the residual silicic melt is controlled by a single dimensionless parameter, the Péclet number (Pe). The Péclet number ratios the advective flux of the buoyant fluid to the diffusion of elements across the melt that surrounds the fluid. We find that at low Pe (i.e., thick magma body, fast diffusion transport or slow ascent of fluid), the enrichment factor between the melt and the fluid

approaches values predicted by partition coefficients. On the other hand for Pe greater or equal to 1, the enrichment factor is significantly reduced (lower than partition coefficient between the MVP and the silicate melt).

[52] The mass flux of metals to the hydrothermal system depends on (1) their enrichment in the fluid phase and (2) the mass flux of metal-rich fluid out of the magma body. Using scaling laws, we show that the extraction and transport of metals out of the magma body is more efficient when the latter reaches high crystallinities (reduces average diffusion length and allows for fluid percolation) as long as the fluid phase can form connected pathways to escape (see also *Shinohara and Hedenquist* [1997] for a similar conclusion). We propose a two-stage model whereby the slow development of capillary channels of exsolved volatiles (MVP) in a crystal-rich mush allow for near equilibrium partitioning of elements between large portions of the residual melt in the mush and the MVP. When these capillary channels achieve percolation through the crystal-rich magmatic system, rapid outgassing allows their transport out of the magma body without much further chemical interactions with it.

[53] The model predicts that efficient metal transfer from magmas to the overlying hydrothermal system requires high crystallinity and high exsolved volatile volume fraction. A mature upper crustal, silicic mush, subject to repeated recharge events, and relatively undisturbed by volcanic eruptions, is therefore the ideal situation to build a large ore deposit. Such a prediction is in agreement with natural observations [*Halter et al.*, 2005] that the bulk of the ore deposits is a late feature that largely post-dates volcanic activity.

[54] The occurrence of brine-vapor separation at shallow depths on the ability to form ore-deposits is widely accepted [*Hedenquist and Lowenstern*, 1994; *Williams-Jones and Heinrich*, 2005], the model we propose offers a simple way to characterize, and a first attempt to quantify, the transport and enrichment of the volatile phase as it leaves the magma chamber. The processes that control the evolution of the MVP and the deposition of metals after the MVP exits the magma body are not treated here. Future studies attempting to couple the metal extraction model we propose here to a thermodynamical model for the deposition of metals as the MVP exits the magma chamber and interacts with an hydrothermal system would provide testable hypotheses to relate geochemical data (enrichment

factor ratios) to volatile transport and elemental mass flux to the hydrothermal system.

## Acknowledgments

[55] C.H. acknowledges funding from NSF-EAR 1144957, O.B. from NSF EAR grant 0809828 and J.D. from NSF-EAR 0948532. The authors would like to thank the editor, one anonymous reviewer and Adam Simon for their helpful comments.

## References

- Bachmann, O., and G. W. Bergantz (2004), On the origin of crystal-poor rhyolites: Extracted from batholithic crystal mushes, *J. Petrol.*, *45*, 1565–1582, doi:10.1093/ptrology/egh019.
- Bachmann, O., and G. W. Bergantz (2008), Rhyolites and their source mushes across tectonic settings, *J. Petrol.*, *49*, 2277–2285, doi:10.1093/ptrology/egn068.
- Bear, J. (1972), *Dynamics of Fluids in Porous Media*, Elsevier, New York.
- Bergantz, G. W., and J. Ni (1999), A numerical study of sedimentation by dripping instabilities in viscous fluids, *Int. J. Multiphase Flow*, *25*(2), 307–320.
- Burnham, C. W. (1979), Magmas and hydrothermal fluids, in *Geochemistry of Hydrothermal Ore Deposits*, vol. 1, edited by H. L. Barnes, pp. 63–75, John Wiley, New York.
- Burnham, C. W. (1985), Energy release in subvolcanic environments; Implications for breccia formation, *Econ. Geol.*, *80*, 1515–1522.
- Candela, P. (1986), Generalized mathematical models for the fractional evolution of vapor from magmas in terrestrial planetary crusts, in *Chemistry and Physics of the Terrestrial Planets*, *Adv. Phys. Geochem.*, *6*, 362–396.
- Candela, P. (1989a), Magmatic ore-forming fluids: Thermodynamic and mass transfer calculations of metal concentrations, in *Ore Deposition Associated With Magma*, *Rev. Econ. Geol.*, vol. 4, pp. 223–233, Soc. of Econ. Geol., El Paso, Tex.
- Candela, P. (1989b), Calculation of magmatic fluid contributions to porphyry-type ore systems: Predicting fluid inclusion chemistries, *Geochem. J.*, *23*, 295–305, doi:10.2343/geochemj.23.295.
- Candela, P. A. (1991), Physics of aqueous phase evolution in plutonic environments, *Am. Mineral.*, *76*(7–8), 1081–1091.
- Candela, P. A. (1997), A review of shallow, ore-related granites: Textures, volatiles, and ore metals, *J. Petrol.*, *38*(12), 1619–1633, doi:10.1093/ptrology/38.12.1619.
- Cardoso, S. S. S., and A. W. Woods (1999), On convection in a volatile-saturated magma, *Earth Planet. Sci. Lett.*, *168*, 301–310, doi:10.1016/S0012-821X(99)00057-6.
- Chung, H.-Y., and J. E. Mungall (2009), Physical constraints on the migration of immiscible fluids through partially molten silicates, with special reference to magmatic sulfide ores, *Earth Planet. Sci. Lett.*, *286*(1–2), 14–22, doi:10.1016/j.epsl.2009.05.041.
- Claußen, O., and C. Rüssel (1998), Diffusivities of polyvalent elements in glass melts, *Solid State Ionics*, *105*, 289–296.
- Cline, J. S., and R. J. Bodnar (1991), Can economic porphyry copper mineralization be generated by a typical calc-alkaline melt?, *J. Geophys. Res.*, *96*(B5), 8113–8126, doi:10.1029/91JB00053.

- Costa, A., S. Blake, and S. Self (2006), Segregation processes in vesiculating crystallizing magmas, *J. Volcanol. Geotherm. Res.*, 153(3–4), 287–300, doi:10.1016/j.jvolgeores.2005.12.006.
- de Silva, S. L., and J. A. Wolff (1995), Zoned magma chambers; The influence of magma chamber geometry on sidewall convective fractionation, *J. Volcanol. Geotherm. Res.*, 65(1–2), 111–118, doi:10.1016/0377-0273(94)00105-P.
- Dufek, J., and O. Bachmann (2010), Quantum magmatism: Magmatic compositional gaps generated by melt-crystal dynamics, *Geology*, 38, 687–690, doi:10.1130/G30831.1.
- Frank, M. R., A. C. Simon, T. Pettke, P. A. Candela, and P. M. Piccoli (2011), Gold and copper partitioning in magmatic-hydrothermal systems at 800°C and 100 MPa, *Geochim. Cosmochim. Acta*, 75, 2470–2482.
- Frezzotti, M., and A. Peccerillo (2004), Fluid inclusion and petrological studies elucidate reconstruction of magma conduits, *Eos Trans. AGU*, 85(16), 157, doi:10.1029/2004EO160001.
- Ghiorso, M. S., and R. O. Sack (1995), Chemical mass transfer in magmatic processes IV: A revised and internally consistent thermodynamic model for the interpolation and extrapolation of liquid-solid equilibria in magmatic systems at elevated temperatures and pressures, *Contrib. Mineral. Petrol.*, 119, 197–212, doi:10.1007/BF00307281.
- Halter, W. E., T. Pettke, and C. A. Heinrich (2002), The origin of Cu/Au ratios in porphyry-type ore deposits, *Science*, 296(5574), 1844–1846, doi:10.1126/science.1070139.
- Halter, W. E., C. A. Heinrich, and T. Pettke (2005), Magma evolution and the formation of porphyry Cu-Au ore fluids: Evidence from silicate and sulfide melt inclusions, *Mineral. Deposita*, 39, 845–863.
- Harris, A. C., V. S. Kamenetsky, N. C. White, E. van Achterbergh, and C. G. Ryan (2003), Melt inclusions in veins: Linking magmas and porphyry Cu deposits, *Science*, 302, 2109–2111, doi:10.1126/science.1089927.
- Hedenquist, J. W., and J. B. Lowenstern (1994), The role of magmas in the formation of hydrothermal ore deposits, *Nature*, 370, 519–527, doi:10.1038/370519a0.
- Heinrich, C. A. (2005), The physical and chemical evolution of low-salinity magmatic fluids at the porphyry to epithermal transition: A thermodynamic study, *Miner. Deposita*, 39(8), 864–889, doi:10.1007/s00126-004-0461-9.
- Hildreth, W. (2004), Volcanological perspectives on Long Valley, Mammoth Mountain, and Mono Craters: Several contiguous but discrete systems, *J. Volcanol. Geotherm. Res.*, 136(3–4), 169–198, doi:10.1016/j.jvolgeores.2004.05.019.
- Huber, C., O. Bachmann, and M. Manga (2009), Homogenization processes in silicic magma chambers by stirring and latent heat buffering, *Earth Planet. Sci. Lett.*, 283, 38–47, doi:10.1016/j.epsl.2009.03.029.
- Hurwitz, S., and O. Navon (1994), Bubble nucleation in rhyolitic melts: Experiments at high pressure, temperature, and water content, *Earth Planet. Sci. Lett.*, 122, 267–280, doi:10.1016/0012-821X(94)90001-9.
- Karlstrom, L., M. L. Rudolph, and M. Manga (2012), Caldera size modulated by the yield stress within a crystal-rich magma reservoir, *Nat. Geosci.*, doi:10.1038/ngeo1453, in press.
- Klugel, A., T. H. Hansteen, and K. Galipp (2005), Magma storage and underplating beneath Cumbre Vieja volcano, La Palma (Canary Islands), *Earth Planet. Sci. Lett.*, 236(1–2), 211–226.
- Koyaguchi, T., and K. Kaneko (1999), A two-stage thermal evolution model of magmas in continental crust, *J. Petrol.*, 40(2), 241–254, doi:10.1093/ptro/40.2.241.
- Lemmon, E. W., M. O. McLinden, and D. G. Friend (2003), Thermophysical properties of fluid systems [online], in *NIST Chemistry WebBook, NIST Stand. Ref. Database*, 69, edited by P. J. Linstrom and W. G. Mallard, Natl. Inst. of Stand. and Technol., Gaithersburg, Md. [Available at <http://webbook.nist.gov/chemistry/>.]
- Linde, A. T., I. S. Sacks, M. J. S. Johnston, D. P. Hill, and R. G. Billam (1994), Increased pressure from rising bubbles as a mechanism for remotely triggered seismicity, *Nature*, 371, 408–410, doi:10.1038/371408a0.
- Lipman, P. W. (2007), Incremental assembly and prolonged consolidation of Cordilleran magma chambers: Evidence from the Southern Rocky Mountain volcanic field, *Geosphere*, 3(1), 42, doi:10.1130/GES00061.1.
- Mangan, M., and T. Sisson (2000), Delayed, disequilibrium degassing in rhyolite magma: Decompression experiments and implications for explosive volcanism, *Earth Planet. Sci. Lett.*, 183(3–4), 441–455, doi:10.1016/S0012-821X(00)00299-5.
- Marsh, B. D. (1981), On the crystallinity, probability of occurrence, and rheology of lava and magma, *Contrib. Mineral. Petrol.*, 78, 85–98, doi:10.1007/BF00371146.
- Marsh, B. D. (1996), Solidification fronts and magmatic evolution, *Mineral. Mag.*, 60, 5–40, doi:10.1180/minmag.1996.060.398.03.
- McBirney, A. R., B. H. Baker, and R. H. Nilson (1985), Liquid fractionation. Part 1: Basic principles and experimental simulations, *J. Volcanol. Geotherm. Res.*, 24, 1–24, doi:10.1016/0377-0273(85)90026-5.
- Muntean, J. L., J. S. Cline, A. C. Simon, and A. A. Longo (2011), Magmatic-hydrothermal origin of Nevada’s Carlin-type gold deposits, *Nat. Geosci.*, 4(2), 122–127.
- Nadeau, O., A. E. Williams-Jones, and J. Stix (2010), Sulphide magma as a source of metals in arc-related magmatic hydrothermal ore fluids, *Nat. Geosci.*, 3(7), 501–505.
- Naldrett, A. J. (2004), *Magmatic Sulfide Deposits: Geology, Geochemistry and Exploration*, Springer, Berlin.
- Nilson, R. H., A. R. McBirney, and B. H. Baker (1985), Liquid fractionation. Part 2: Fluid dynamics and quantitative implications for magmatic systems, *J. Volcanol. Geotherm. Res.*, 24, 25–54.
- Parmigiani, A., C. Huber, B. Chopard, and O. Bachmann (2011), Pore-scale mass and reactant transport in multiphase porous media flows, *J. Fluid Mech.*, 686, 40–76, doi:10.1017/jfm.2011.268.
- Phillips, J. C., and A. W. Woods (2002), Suppression of large-scale magma mixing by melt-volatile separation, *Earth Planet. Sci. Lett.*, 204, 47–60, doi:10.1016/S0012-821X(02)00978-0.
- Philpotts, A. R., J. Shi, and C. Brustman (1998), Role of plagioclase crystal chains in the differentiation of partly crystallized basaltic magma, *Nature*, 395, 343–346, doi:10.1038/26404.
- Rudnick, R. L., and S. Gao (2003), The composition of the continental crust, in *Treatise on Geochemistry*, vol. 3, *The Crust*, edited by R. L. Rudnick, pp. 1–64, Elsevier, Amsterdam.
- Ruprecht, P., G. W. Bergantz, and J. Dufek (2008), Modeling of gas-driven magmatic overturn: Tracking of phenocryst dispersal and gathering during magma mixing, *Geochem. Geophys. Geosyst.*, 9, Q07017, doi:10.1029/2008GC002022.
- Saffman, P. G., and G. Taylor (1958), The penetration of a fluid into a porous medium or Hele-Shaw cell containing a more viscous liquid, *Proc. R. Soc. London, Ser. A*, 245(1242), 312–329, doi:10.1098/rspa.1958.0085.
- Scaillet, B. (2010), Economic geology: Volatile destruction, *Nat. Geosci.*, 3(7), 456–457, doi:10.1038/ngeo908.
- Shinohara, H., and J. W. Hedenquist (1997), Constraints on magma degassing beneath the Far Southeast porphyry

- Cu-Au deposit, Philippines, *J. Petrol.*, *38*(12), 1741–1752, doi:10.1093/ptro/38.12.1741.
- Sierou, A., and J. R. Lister (2003), Self-similar solutions for viscous capillary pinch-off, *J. Fluid Mech.*, *497*, 381–403, doi:10.1017/S0022112003006736.
- Sillitoe, R. H. (2010), Porphyry copper systems, *Econ. Geol.*, *105*(1), 3–41, doi:10.2113/gsecongeo.105.1.3.
- Simon, A. C., M. R. Frank, T. Pettke, P. A. Candela, P. M. Piccoli, and C. A. Heinrich (2005), Gold partitioning in melt-vapor-brine systems, *Geochim. Cosmochim. Acta*, *69*, 3321–3335.
- Simon, A. C., P. Candela, P. Piccoli, and L. Engländer (2008), The effect of crystal–melt partitioning on the budgets of copper, gold, and silver, *Am. Mineral.*, *93*, 1437–1448, doi:10.2138/am.2008.2812.
- Taran, Y. A., A. Bernard, J.-C. Gavilanes, and F. Africano (2000), Native gold in mineral precipitates from high-temperature volcanic gases of Colima volcano, Mexico, *Appl. Geochem.*, *15*(3), 337–346, doi:10.1016/S0883-2927(99)00052-9.
- Vignerresse, J. L. (2007), The role of discontinuous magma inputs in felsic magma and ore generation, *Ore Geol. Rev.*, *30*(3–4), 181–216, doi:10.1016/j.oregeorev.2006.03.001.
- Vignerresse, J.-L., P. Barbey, and M. Cuney (1996), Rheological transitions during partial melting and crystallization with application to felsic magma segregation and transfer, *J. Petrol.*, *37*(6), 1579–1600, doi:10.1093/ptrology/37.6.1579.
- von der Gönna, G., and C. Rüssel (2000), Diffusivities of polyvalent elements in a  $15\text{Na}_2\text{O} \cdot 85\text{SiO}_2$  glass melt, *J. Non Cryst. Solids*, *272*, 139–146.
- Walsh, S. D. C., and M. O. Saar (2008), Numerical models of stiffness and yield stress growth in crystal–melt suspensions, *Earth Planet. Sci. Lett.*, *267*(1–2), 32–44, doi:10.1016/j.epsl.2007.11.028.
- Webster, J. D., C. M. Tappen, and C. W. Mandeville (2009), Partitioning behavior of chlorine and fluorine in the system apatite–melt–fluid. II: Felsic silicate systems at 200 MPa, *Geochim. Cosmochim. Acta*, *73*(3), 559–581, doi:10.1016/j.gca.2008.10.034.
- Williams, T. J., P. A. Candela, and P. M. Piccoli (1995), The partitioning of copper between silicate melts and two-phase aqueous fluids: An experimental investigation at 1 kbar, 800°C and 0.5 kbar, 850°C, *Contrib. Mineral. Petrol.*, *121*(4), 388–399, doi:10.1007/s004100050104.
- Williams-Jones, A. E., and C. A. Heinrich (2005), Vapor transport and the formation of magmatic-hydrothermal ore deposits, *Econ. Geol.*, *100*, 1287–1312.
- Zajacz, Z., W. E. Halter, T. Pettke, and M. Guillong (2008), Determination of fluid/melt partition coefficients by LA-ICPMS analysis of co-existing fluid and silicate melt inclusions: Controls on element partitioning, *Geochim. Cosmochim. Acta*, *72*, 2169–2197.
- Zelenski, M., and S. Bortnikova (2005), Sublimate speciation at Mutnovsky volcano, Kamchatka, *Eur. J. Mineral.*, *17*(1), 107–118, doi:10.1127/0935-1221/2005/0017-107.
- Zhang, W. W., and J. R. Lister (1999), Similarity solutions for capillary pinch-off in fluids of different viscosity, *Phys. Rev. Lett.*, *83*, 1151–1154, doi:10.1103/PhysRevLett.83.1151.
- Zhang, Y., and D. J. Cherniak (2010), Diffusion in minerals and melts: Theoretical background, in *Diffusion in Minerals and Melts*, edited by Y. Zhang and D. J. Cherniak, *Rev. Mineral. Geochem.*, *72*, 5–59, doi:10.2138/rmg.2010.72.2.